Supplementary Material (ESI) for Energy & Environmental Science

Modeling and Simulation of Nuclear Fuel Materials

Ram Devanathan,[1,*] Laurent Van Brutzel,[2] Alain Chartier,[2] Christine Guéneau,[2] Ann E. Mattsson,[3] Veena Tikare,[3] Timothy Bartel,[3] Theodore Besmann,[4] Marius Stan,[5] and Paul Van Uffelen[6]

[1]Pacific Northwest National Laboratory, Richland, WA 99352, USA

[2] CEA, Service de Chimie Physique, F-91191 Gif-sur-Yvette, France

[3]Sandia National Laboratories, Albuquerque, NM, USA

[4]Oak Ridge National Laboratory, Oak Ridge, TN, USA

[5]Los Alamos National Laboratory, Los Alamos, NM, USA

[6]Institute for Transuranium Elements, Karlsruhe, Germany

Supplementary Online Information

1. The Relativistic Kohn-Sham equations

The relativistic Kohn-Sham equations have been discussed by Dreizler and Gross.[1]

Their equations can be expressed as follows:

$$\left(c\,\boldsymbol{\alpha}\cdot\left(\boldsymbol{p}-\frac{e\boldsymbol{A}_{\mathit{eff}}}{c}\right)+\begin{pmatrix} I & 0 \\ 0 & I \end{pmatrix} V_{\mathit{eff}}(\boldsymbol{r})+\beta\, mc^2\right)\psi_n(\boldsymbol{r}) = E_n\,\psi_n(\boldsymbol{r}) \tag{1}$$

with

$$V_{\mathit{eff}}(\boldsymbol{r}) \;=\; -e\left(A^0_{ext}(\boldsymbol{r})+\int d^3r'\frac{J^0(\boldsymbol{r'})}{|\boldsymbol{r}-\boldsymbol{r'}|}+\frac{\delta E_{xc}[J^\mu]}{\delta J^0(\boldsymbol{r})}\right) \tag{2}$$

and

$$e\boldsymbol{A}_{\mathit{eff}}(\boldsymbol{r}) = -e\left(\boldsymbol{A}_{ext}(\boldsymbol{r}) + \int d^3r' \frac{\boldsymbol{J}(\boldsymbol{r}')}{|\boldsymbol{r}-\boldsymbol{r}'|} + \frac{\delta E_{xc}[J^\mu]}{\delta \boldsymbol{J}(\boldsymbol{r})}\right), \tag{3}$$

for all negative and positive energy orbitals. Note that the energy includes the rest mass energy, and that the available energy for bonding and kinetic energy is $E_n - mc^2$.

The matrices are defined as

$$\alpha_k = \begin{pmatrix} 0 & \sigma_k \\ \sigma_k & 0 \end{pmatrix} \qquad \beta = \begin{pmatrix} I & 0 \\ 0 & -I \end{pmatrix} \qquad I = \begin{pmatrix} 1 & 0 \\ 0 & 1 \end{pmatrix} \tag{4}$$

and σ_k denotes the Pauli matrices. The Dirac 4-component spinors, ψ_n, can be represented as single-row matrices:

$$\psi_n = \begin{pmatrix} \psi_{1,n} \\ \psi_{2,n} \\ \psi_{3,n} \\ \psi_{4,n} \end{pmatrix} = \begin{pmatrix} \psi_{A,n} \\ \psi_{B,n} \end{pmatrix}. \tag{5}$$

The conserved current, $J^\mu = (J^0, \boldsymbol{J})$, is analogous to the density in non-relativistic DFT, and is thus the conserved current of the real system that can be calculated from the above spinor solutions to the relativistic KS equations:

$$J^\mu = (J^0, \boldsymbol{J}) = -e\sum_n \left(\psi_n^\dagger \psi_n, \psi_n^\dagger \boldsymbol{\alpha}\, \psi_n\right). \tag{6}$$

It is well known that the vacuum expectation value of the current operator is non-zero; pairs of electron-positrons can spontaneously be created in vacuum, which is referred to as vacuum polarization. If this vacuum polarization is neglected, the current becomes[1]:

$$J^{\mu} = -e \sum_{-mc^2 < E_n < E_F} \left(\psi_n^{\dagger}\psi_n, \psi_n^{\dagger}\boldsymbol{\alpha}\,\psi_n\right) . \tag{7}$$

2. From the Dirac equation to the Schrödinger equation

We can separate the compact equation for the bi-spinor ψ_n in Equation 1, into two equations for the 2-component spinors $\psi_{A,n}$ and $\psi_{B,n}$:

$$\left[\boldsymbol{\sigma}\cdot\left(\boldsymbol{p}-\frac{e\boldsymbol{A}_{eff}}{c}\right)\right]\psi_{B,n}(\boldsymbol{r}) = \frac{1}{c}\left(E_n - V_{eff}(\boldsymbol{r}) - mc^2\right)\psi_{A,n}(\boldsymbol{r}) \tag{8}$$

$$\left[\boldsymbol{\sigma}\cdot\left(\boldsymbol{p}-\frac{e\boldsymbol{A}_{eff}}{c}\right)\right]\psi_{A,n}(\boldsymbol{r}) = \frac{1}{c}\left(E_n - V_{eff}(\boldsymbol{r}) + mc^2\right)\psi_{B,n}(\boldsymbol{r}) . \tag{9}$$

We can now eliminate the lower component spinor and for the upper component spinor, we obtain

$$\left[\boldsymbol{\sigma}\cdot\left(\boldsymbol{p}-\frac{e\boldsymbol{A}_{eff}}{c}\right)\right]\frac{c^2}{E_n - V_{eff}(\boldsymbol{r}) + mc^2}\left[\boldsymbol{\sigma}\cdot\left(\boldsymbol{p}-\frac{e\boldsymbol{A}_{eff}}{c}\right)\right]\psi_{A,n}(\boldsymbol{r}) = \left(E_n - V_{eff}(\boldsymbol{r}) - mc^2\right)\psi_{A,n}(\boldsymbol{r}) , \tag{10}$$

while the equation for the lower component spinor becomes

$$\psi_{B,n}(\boldsymbol{r}) = \frac{c}{E_n - V_{eff}(\boldsymbol{r}) + mc^2}\left[\boldsymbol{\sigma}\cdot\left(\boldsymbol{p}-\frac{e\boldsymbol{A}_{eff}}{c}\right)\right]\psi_{A,n}(\boldsymbol{r}) . \tag{11}$$

In the non-relativistic limit,

$$E_n \approx mc^2 , \tag{12}$$

and we can define a non-relativistic energy as

$$E_n^{(NR)} = E_n - mc^2 , \tag{13}$$

which thus is a small energy. If $V_{eff}(r)$ is also small compared to $2mc^2$, we can expand

$$\frac{c^2}{E_n - V_{eff}(\boldsymbol{r}) + mc^2} = \frac{1}{2m}\left[1 - \frac{E_n^{(\mathrm{NR})} - V_{eff}(\boldsymbol{r})}{2mc^2} + \cdots\right]. \tag{14}$$

If only the first term in the expansion of Equation (14) is retained, Equation (10) becomes the non-relativistic Schrödinger equation

$$\left[\frac{1}{2m}\left(\boldsymbol{p} - \frac{e\boldsymbol{A}_{eff}}{c}\right)^2 - \frac{e\hbar}{2mc}\boldsymbol{\sigma}\cdot\boldsymbol{B} + V_{eff}(\boldsymbol{r})\right]\psi_{A,n} = E_n^{(\mathrm{NR})}\psi_{A,n} , \tag{15}$$

and we note that

$$\psi_{B,n} \propto \frac{v}{c}\psi_{A,n} , \tag{16}$$

that is, in the non-relativistic limit, $\psi_{B,n}$, the *small* component, is much smaller than $\psi_{A,n}$, the *large* component, and can be neglected.

Retaining also the second term in the expansion in Equation (14), results in the non-relativistic Schrödinger equation with first order relativistic corrections, such as, the spin-orbit coupling.

3. When do we need to use the full relativistic equation?

The assumption made above, restricting the range of validity of the non-relativistic treatment of electrons, is:

$$|E_n^{(\mathrm{NR})} - V_{eff}(\boldsymbol{r})| << 2mc^2 \quad (17)$$

For typical nuclear fuel calculations the atomic core regions with high density are the regions of interest. Here $V_{ext}(r)$ can become very large, resulting in large effective potentials, $V_{eff}(r)$, as shown in Figure S1. While the energy levels (a global property) for the hydrogen-like ion do not differ much when calculated with the relativistic and non-relativistic equations, see Figure S2, local properties, such as wave functions, can be influenced in the regions of space near the nuclei where the effective potential is highly attractive, and the assumption in Equation (17) is violated.

By examining the behavior of the wave functions of the hydrogen-like ions close to the nuclei, that is, examining the exact solutions to the hydrogen-like ion as $r \rightarrow 0$, we can explore the differences between a Dirac and a Schrödinger equation treatment. In many DFT codes, for example the RSPt code,[2] equations by Harmon and Koelling, including scalar relativistic corrections, are used, and we therefore also include these in our comparison. The radial dependence of the wave functions in the Dirac, the scalar relativistic, and the Schrödinger equations respectively are:

Schrödinger equation: r^l, (18)

Scalar relativistic: $r^{\sqrt{l(l+1)+1-(Z\alpha)^2}-1}$, (19)

and Dirac equation: $r^{\sqrt{\kappa^2-(Z\alpha)^2}-1}$, (20)

where $\alpha \approx 1/137$ is the fine structure constant. Already for the $s_{1/2}$ states ($l = 0$ and $\kappa = -1$) we see a difference: while the Schrödinger equation gives that the radial function tends to a finite value at the origin, the relativistic treatment, even on the scalar level, gives a slight divergence since $\sqrt{1-(Z\alpha)^2}-1 < 0$. This mild singularity, however, is of academic interest only, since the wave function at short distances must be modified because of the finite charge distribution of the nucleus.

For states with $l > 0$ and $|\kappa| > 1$ all treatments give wave functions that tend to zero at the origin.

However, the $\kappa = 1$ states, that is, the $p_{1/2}$ states, have different behavior in the different treatments. While the Dirac treatment gives the same slight divergence, discussed above, as the $s_{1/2}$ states, the scalar relativistic and Schrödinger equation both give wave functions that tend to zero. It is believed that this erroneous behavior of the $p_{1/2}$-state in the Schrödinger and scalar relativistic treatments is at fault for part of the failure of DFT calculations to give correct lattice constants for actinides (the other reason being insufficiently accurate exchange-correlation functionals). In Figure 4 in the main article, the difference in behavior is made evident for the $6p_{1/2}$-state.

4. Using non-relativistic (NR) exchange-correlation functionals

In non-relativistic DFT, the currents $\boldsymbol{J} = -e\sum \psi_n^\dagger \boldsymbol{\alpha} \psi_n$, that couple to the effective vector potential A_{eff} in the Hamiltonian in Equation (1), are not used, and in order to connect to, and be able to use functionals created for NR DFT, we would rather use the spin-density

$$\boldsymbol{S} = -\sum_{-mc^2<E_n<E_F} \psi_n^\dagger \beta \boldsymbol{\Sigma} \psi_n \quad . \tag{21}$$

Here

$$\Sigma_k = \begin{pmatrix} \sigma_k & 0 \\ 0 & \sigma_k \end{pmatrix} . \tag{22}$$

For time-independent problems, $\boldsymbol{J}$ can be written as (Gordon decomposition):

$$\boldsymbol{J} = \boldsymbol{I} + \mu_B \nabla \times \boldsymbol{S} \quad . \tag{23}$$

where

$$\boldsymbol{I} = \frac{e}{2mc} \sum_{-mc^2<E_n<E_F} \left\{ \psi_n^\dagger \beta \left[\left(\boldsymbol{p} - \frac{e\boldsymbol{A}_{eff}}{c} \right) \psi_n \right] + \left[\left(\boldsymbol{p} - \frac{e\boldsymbol{A}_{eff}}{c} \right) \psi_n \right]^\dagger \beta \psi_n \right\} . \tag{24}$$

By neglecting the orbital current, $\boldsymbol{I}$, and only using the spin-density current, the $e\,\boldsymbol{\alpha} \cdot A_{eff,}$ in the Hamiltonian in Equation 1 can be simplified and the Hamiltonian becomes

$$\left(c\,\boldsymbol{\alpha} \cdot \boldsymbol{p} + \mu_B \beta \boldsymbol{\Sigma} \cdot \boldsymbol{B}_{eff} + \begin{pmatrix} I & 0 \\ 0 & I \end{pmatrix} V_{eff}(\boldsymbol{r}) + \beta mc^2 \right) \psi_n(\boldsymbol{r}) = E_n\, \psi_n(\boldsymbol{r}) \quad , \tag{25}$$

where $\boldsymbol{B} = \nabla$ x $\boldsymbol{A}$ and μ_B is the Bohr magneton. Equation (3) should be replaced by

$$\mu_B \boldsymbol{B}_{eff}(\boldsymbol{r}) = \left(\mu_B \boldsymbol{B}_{ext}(\boldsymbol{r}) + \int d^3r' \frac{\boldsymbol{M}(\boldsymbol{r}')}{|\boldsymbol{r} - \boldsymbol{r}'|} + \frac{\delta E_{xc}[J^0, M]}{\delta \boldsymbol{M}(\boldsymbol{r})} \right) , \tag{26}$$

where $\boldsymbol{M} = \mu_B\, \boldsymbol{S}$.

Usual spin density functional such as LSDA can now be used in a framework that approximately retains the fully relativistic treatment of the Dirac equation.

References

1. R. M. Dreizler and E. K. U. Gross, *Density Functional Theory: An Approach to the Quantum Many-Body Problem*, Springer-Verlag, Berlin, 1990.
2. http://www.rspt.net

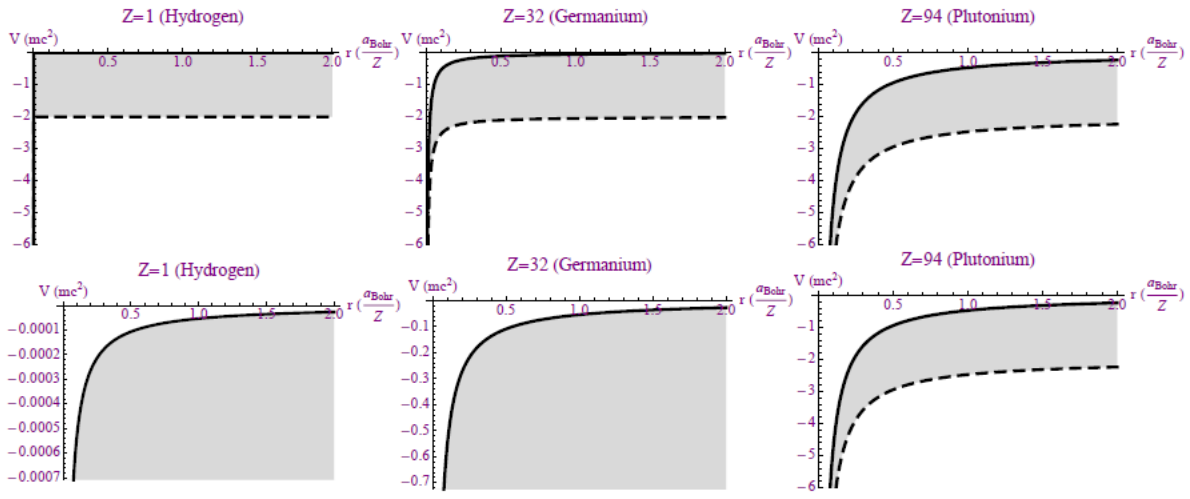

Fig. S1. The Coulomb potential for the hydrogen like atom. The solid line is the electron potential while the dashed line is the positron potential, $2mc^2$ below the electron one. Non-

relativistic calculations show that the average displacement of the electron from the nucleus in the hydrogen-like ion, in units of a_{Bohr}/Z, is $(3n^2 - l(l+1))/2$, motivating the x-axis. The upper row has the same scale on the y-axis, while in the lower row the y-axis has been adjusted so that the electron potentials are similar.

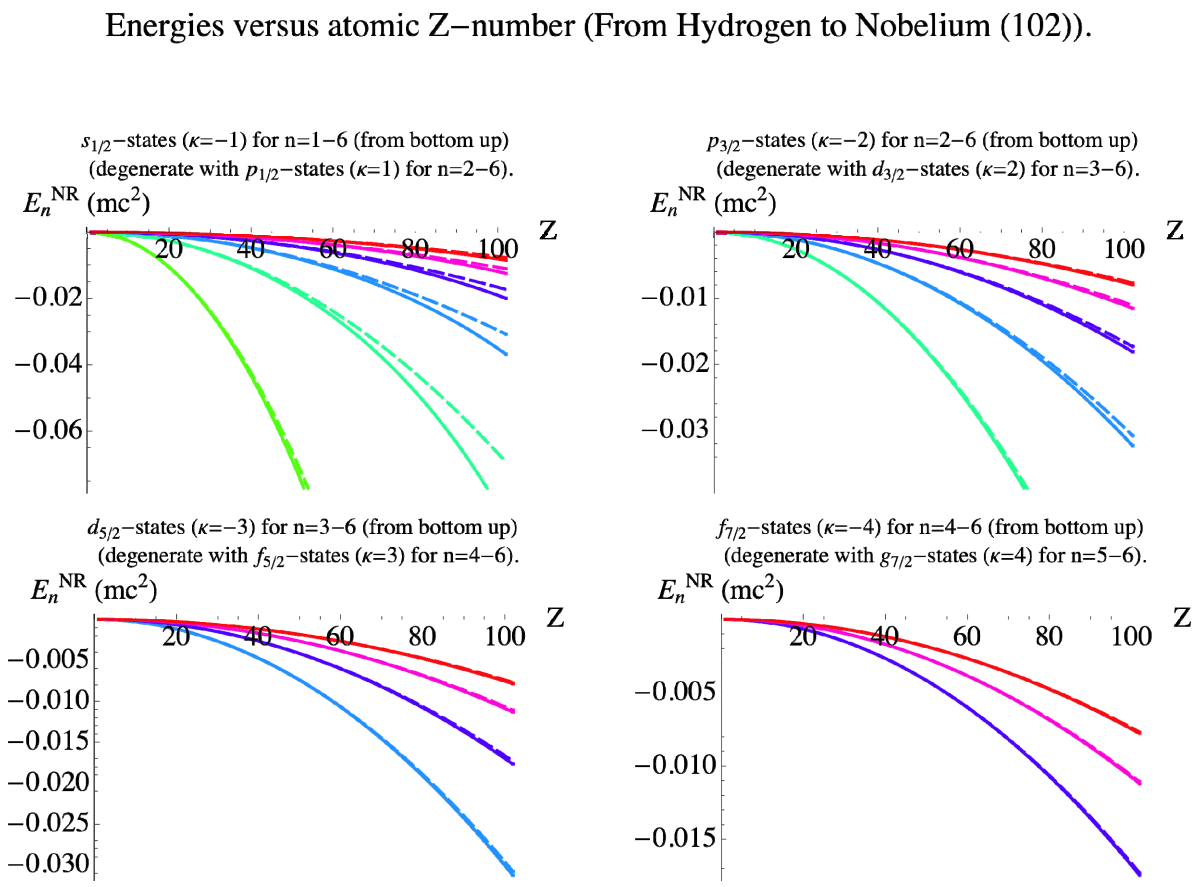

Fig. S2. The energy levels for the hydrogen-like atom versus atomic number Z, as calculated with the Dirac equation and the Schrödinger equation. Full lines are relativistic energies, while the dashed lines are the corresponding energies from the non-relativistic equation.